Accepted Manuscript

A technical method to improve NO_x/NH_3 mixing ratio in SCR system and its engineering applications

Guofu Liu, Yidong Cui, Jiaqing Ji, Dekui Shen, Qi Wang, Chao Li, Kai Hong Luo

PII: S1743-9671(18)31061-4

DOI: https://doi.org/10.1016/j.joei.2018.12.005

Reference: JOEI 546

To appear in: *Journal of the Energy Institute*

Received Date: 8 November 2018

Revised Date: 6 December 2018

Accepted Date: 11 December 2018

Please cite this article as: G. Liu, Y. Cui, J. Ji, D. Shen, Q. Wang, C. Li, K.H. Luo, A technical method to improve NO_x/NH_3 mixing ratio in SCR system and its engineering applications, *Journal of the Energy Institute*, https://doi.org/10.1016/j.joei.2018.12.005.

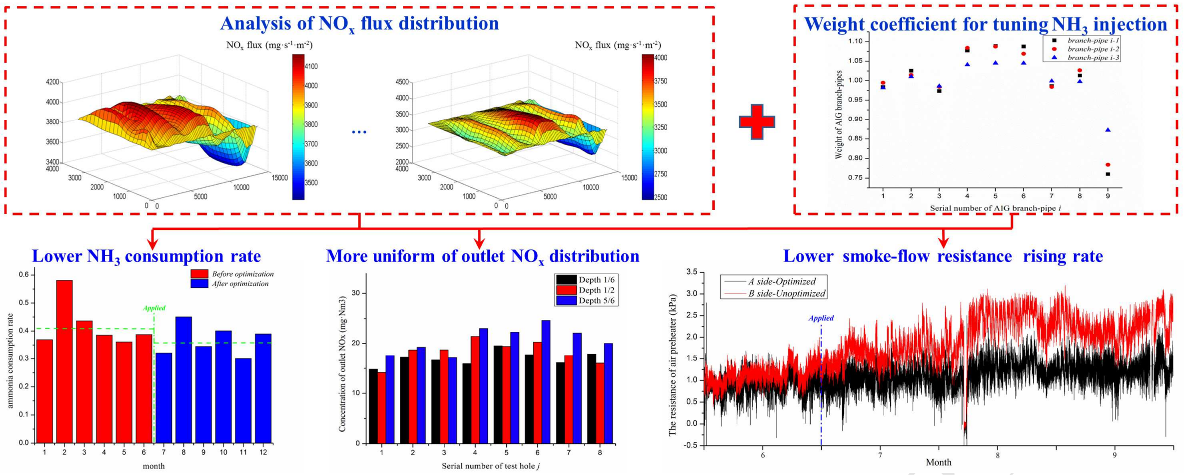

Analysis of NO_x flux distribution
Weight coefficient for tuning NH_3 injection
Lower NH_3 consumption rate
More uniform of outlet NO_x distribution
Lower smoke-flow resistance rising rate

A technical method to improve NO_x/NH_3 mixing ratio in SCR system and its engineering applications

Guofu Liu[a], Yidong Cui[a], Jiaqing Ji[b], Dekui Shen[a, *], Qi Wang[b, c], Chao Li[d], Kai Hong Luo[e]

[a] Key Laboratory of Energy Thermal Conversion and Control of Ministry of Education, School of Energy and Environment, Southeast University, Nanjing 210096, Jiangsu, China

[b] School of measurement and testing engineering, China Jiliang University, Hangzhou 310018, Zhejiang, China

[c] Nanjing Automatic Instrument Automation Co., Ltd, Nanjing 21111, Jiangsu, China

[d] Nanjing Beyond Environmental Engineering Co., Ltd, Nanjing 21111, Jiangsu, China

[e] Department of Mechanical Engineering, University College London, London WC1E 7JE, UK

Abstract:

A technical method for diagnosing the distribution of NO_x flux within the cross-section area in front of ammonia injection grid (AIG) was proposed for guiding the valve-tuning of AIG branch-pipes, in order to optimize the NO_x/NH_3 mixing ratio in the selective catalytic reduction (SCR) system of power plant. The weight coefficient of each branch-pipe in AIG system can be quantitatively determined with regard to the distribution of NO_x flux in the corresponding sub-zone of the cross-section area. The control strategy of the valves for different AIG branch-pipes can be achieved for guiding the NH_3 injection and improving the NO_x/NH_3 mixing ratio within the whole cross-section area in front of AIG. The technology has been applied on one side of the SCR system flue-gas tunnels (normally two tunnels for the SCR system called as A-side and B-side) of a 660 MW plant for more than one year. The ammonia consumption rate of the SCR system was reduced about 12.62% and the uniformity of outlet NO_x distribution was estimated to be greatly improved by about 79.01% with regard to the standard deviation. The rising rate of the flue gas resistance of the air preheater was slown down by 39.18% compared to that of the other flue-gas tunnel of SCR system. This implied that the formation of the sticky ammonium bisulfate (ABS) on air preheater was significantly inhibited through the application of this technology.

Key Words: SCR system, NO_x flux distribution, ammonia injection, flue gas resistance; ammonium bisulfate

1. Introduction

Selective catalytic reduction (SCR) technology is playing an important role in NO_x removal of the coal-fired power plant [1-3]. Real-time denitrification performance of a running SCR system would be more affected by operational parameters instead of the catalyst activity as the core parameter of SCR system design [4-6]. A retrofit project of ultra-low emission of NO_x was being forced to proceed for coal-fired power plant in China [7,8]. The oxidation property of SCR system was greatly enhanced due to the newly added layer of denitrification catalyst, resulting in the increase of SO_3 concentration at the exit of the SCR system [9,10]. The amount of the escaped ammonia should be strictly limited to avoid the formation of ammonium bisulfate (ABS), which is the vital factor to the flue gas resistance of air preheater and the safe operation of the power plant [11,12].

* Corresponding author: Dekui Shen, E-mail: 101011398@seu.edu.cn.

The denitrification performance of SCR system can be greatly influenced by the NO_x/NH_3 mixing ratio [13-15]. The distribution of NO_x concentration within flue gas was quite uneven for the instability of low nitrogen combustion in boiler[16,17]. Besides that, the velocity of flue gas was also found to be uneven owing to the adjustment of boiler load, the changes of flue structure and so on[18,19]. The accurate flux of the NO_x flowing can be described by the index of NO_x flux, which can be obtained from the product of NO_x concentration and the velocity of flue gas. The NO_x flux in the sub-zone of the cross-section area in front of ammonia injection grid (AIG) varied with space and time. The total amount of NH_3 was roughly equally distributed in AIG system regardless of the non-uniform characteristic of NO_x flux for most coal-fired plants[20]. Consequently, the amount of ammonia escape would significantly increase in order to meet the strict emission standards within those all sub-zones of the cross-section area. Sticky ABS (liquid phase) was greatly formed at the cold-side of air preheater, leading to the increase of the flue gas resistance of air preheater[21,22].

The partition-controlled AIG system was widely used owing to its potential of NO_x/NH_3 mixing ratio tuning [23]. The amount of ammonia injected for the sub-unit of AIG system could be independently tuned though the corresponding valve installed on the AIG branch-pipes. The NO_x/NH_3 mixing ratio in SCR system could be adjusted for achieving the ideal matching of the amount of NH_3 injection and NO_x flux and minimizing the amount of ammonia escape. However, the strategy for tuning the valves of AIG branch-pipes to gain the optimal NO_x/NH_3 mixing ratio is insufficiently reported in the literature.

A technical method for diagnosing the distribution of NO_x flux within the cross-section area in front of AIG was proposed for guiding the valve tuning of AIG branch pipes, in order to optimize the NO_x/NH_3 mixing ratio in the SCR system of power plant. The weight coefficient of each branch-pipe in AIG system can be quantitatively determined with regard to the distribution of NO_x flux in the sub-zone of the cross-section area designated to the branch-pipes. The control strategy of the valves for different AIG branch-pipes can be achieved for guiding the NH_3 injection and improving the NO_x/NH_3 mixing ratio within the whole cross-section area in front of AIG. The proposed technology has been applied on one side of the SCR system of the 660 MW plant, exhibiting the ability for tuning the NO_x/NH_3 mixing ratio.

2. Methods

2.1. The AIG structure of SCR system

With the assistance of the NH_3 injected, the NO_x in flue gas was removed and converted to the harmless nitrogen in the presence of denitrification catalyst. The chemical reactions involved could be described as Eq. (1)~(4) [24]. However, studies have shown that the proportion of NO in the flue gas was about 95%, and it is generally recognized that the critical denitrification path can be characterized by Eq. (1)[25,26]. That is to say the SCR system would be maintained efficiently and safely when the NO_x/NH_3 mixing ratio was tuned at 1:1, instead of resulting in more ammonia escape or excessive emissions of NO_x.

$$4NO + 4NH_3 + O_2 \rightarrow 4N_2 + 6H_2O \quad (1)$$

$$6NO + 4NH_3 \rightarrow 5N_2 + 6H_2O \quad (2)$$

$$6NO_2 + 8NH_3 \rightarrow 7N_2 + 12H_2O \quad (3)$$

$$2NO_2 + 4NH_3 + O_2 \rightarrow 3N_2 + 6H_2O \quad (4)$$

The SCR system belonged to a 660MW subcritical, tangentially-firing pulverized-coal boiler was studied here, which could be shown in Fig. 1. At each corner of the furnace, there are six layers of low NOx burners with over fire air (OFA) arranged at the top. The NO_x involved in the flue gas coming from the economizer and the NH_3 injected through the AIG system consist of 27 sub-units were fully mixed rely on the static mixer applied, several flue turns and so on. Then the denitrification reaction was orderly carried out in the catalyst area bringing about the removal of NO_x pollutants. The NO_x flux in the cross-section A, which was located in front of AIG system, should be further studied because of its non-uniform distribution characteristics.

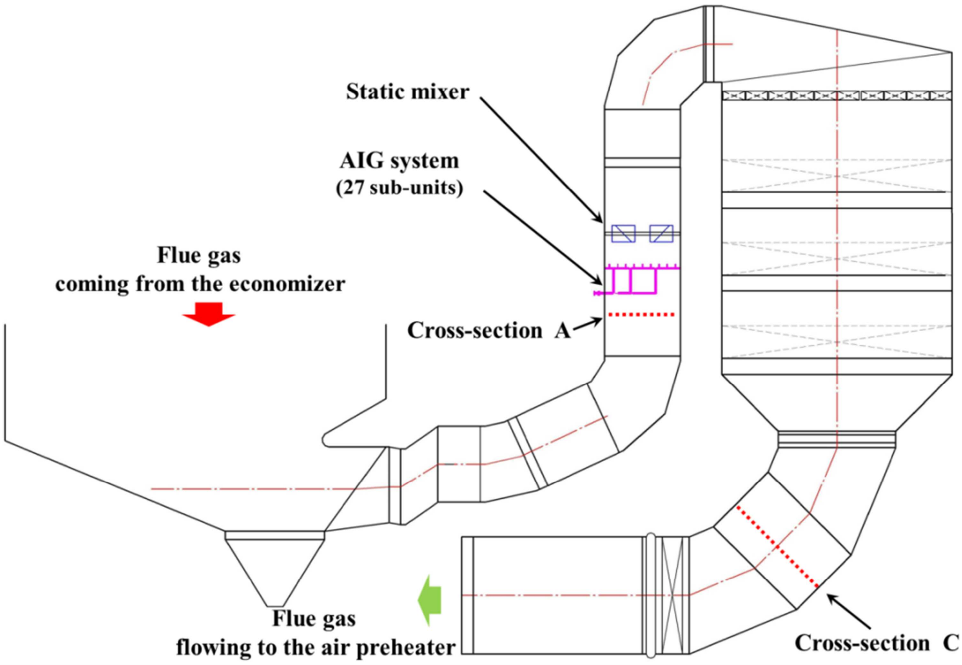

Fig. 1. Schematics of the SCR system

The partition-controlled AIG system with 27 sub-units was adopted in the SCR system of the case work. These 27 sub-units could be divided into 9 identical groups which was respectively made up of 3 different inject sub-units. The mixture of NH_3 and dilution air was injected to the flue by the above 27 sub-units, and the injection amount of each sub-unit could be independently tuned though the corresponding butterfly valve installed on the AIG branch-pipes. Moreover, the cross-section A could be hypothetically divided into 27 sub-zones in line with the 27 sub-units of AIG system, which could be shown in Fig. 2.

Fig. 2. The partition-controlled AIG system.

The hypothetical partitioning method for specific cross-section is closely related to the controlled area of each AIG sub-unit, depending on the structural characteristics of the AIG system, such as the number and the location of these sub-units and so on. The opening of the 27 butterfly valves should be tuned according to the NO_x flux distribution characteristics within each corresponding sub-zones, achieving the better NO_x/NH_3 mixing ratio in the SCR system.

2.2. Acquisition and evaluation of the NO_x flux distribution

The distribution characteristics of NO_x flux in the cross-section A could be obtained through the 13 temporary test holes available, where 3 measuring depths were designed for each temporary test hole. The distribution characteristics of NO_x concentration in the cross-section C, which was located at the exit of SCR system, could also be obtained on basis of the 8 available temporary test holes. The dimensionless depth of above 3 measuring depths in the cross-section A/C was 1/6, 1/2, 5/6, respectively.The NO_x concentration and the velocity of flue gas should be separately measured on each discrete-node firstly. The measurement of the velocity was realized by using a micro pressure gauge and a pitot tube of S type with a correction factor of 0.85, and the NO_x volume concentration was carried out through the Testo 350 flue gas analyzer.

The index of standard deviation was adopted to evaluate the uniformity of the NO_x flux distribution, which could be shown as Eq. (5)[27].

$$C_v = \frac{\sqrt{\sum_{j=1}^{n}(x_j-\bar{x})^2/(n-1)}}{\bar{x}} \times 100\% \quad (5)$$

where C_v, x_j, $\bar{x}$, n represented the standard deviation, the NO_x flux of discrete-node j, the mean of NO_x flux in the cross-section area studied and the number of discrete-node, respectively.

2.3. Analytic method of AIG branch-pipe weight coefficient

The NO_x/NH_3 mixing ratio in SCR system would be optimized through the diagnose of NO_x flux distribution which was reflected by the AIG branch-pipe weight coefficient. The weight coefficient of each branch-pipe in AIG system under a steady load condition could be quantificationally determined with regard to the distribution of NO_x flux in the corresponding sub-zone of the cross-section A, which can be described as Eq. (6)[23].

$$\varphi_i^\tau = f_i^\tau / f_{mean}^\tau \quad (6)$$

where φ_i^τ, f_i^τ, f_{mean}^τ represented the weight coefficient of branch-pipe i under steady load condition of τ, the NO_x flux within the sub-zone of cross-section A controlled by branch-pipe i under steady load condition of τ and the mean of NO_x flux in the whole cross-section A under steady load condition of τ, respectively.

Spatial variation of the NO_x flux in each sub-zone of cross-section A was featured via the index of φ_i^τ. The NO_x flux would also varied with load condition adjustment. Accordingly, the global weight coefficient of each branch-pipe in AIG system could be obtained based on the following principles, which could be shown as Eq. (7).

$$\varphi_i = \sum \varphi_i^\tau \frac{\Delta T^\tau}{\Delta T} \quad (7)$$

where φ_i, ΔT^τ, ΔT represented the global weight coefficient of branch-pipe i, the time period of load condition of τ and the total sample time studied, respectively.

It can be inferred that the variation of NO_x flux in the sub-zone with space and time could be described in line with the index of φ_i. The opening of AIG valves installed on each branch-pipe should be adjusted accordingly based on the weight coefficient differences. The corresponding relationship between the weight coefficient and the valve opening could be described as Eq. (8).

$$ON_i = ON_{max} + \frac{\varphi_i - \varphi_{max}}{\zeta} \quad (8)$$

where ON_i , ON_{max} , φ_{max}, ζ represented the opening of AIG branch-pipe valve *i*, the maximum opening of all AIG branch-pipe valves, the maximum weight coefficient of all AIG branch-pipe and and the compression coefficient, respectively.

The compression coefficient ζ introduced here was an empirical coefficient related to the maximum weight coefficient, the minimum weight coefficient and the extremum of expected opening for all branch-pipe valves. The opening of these branch-pipe valves would be kept within a reasonable range.

3. Results and discussion

3.1. The diagnose of NO_x flux distribution within key cross-section area

3.1.1 Analysis of the NO_x flux distribution for within cross-section A

The test work of the NO_x concentration and the velocity of flue gas within cross-section A was conducted rely on the 13 temporary test holes available under 3 sets of stable load conditions including 300, 450 and 580MW as shown in Fig. 3(a)~(c). Apparently the NO_x flux distribution of each condition within cross-section A had showed distinct inhomogeneity. Furthermore, the standard deviation of NO_x flux distribution under the above load conditions was calculated to be 25.24%, 21.98%, 20.23%, respectively.

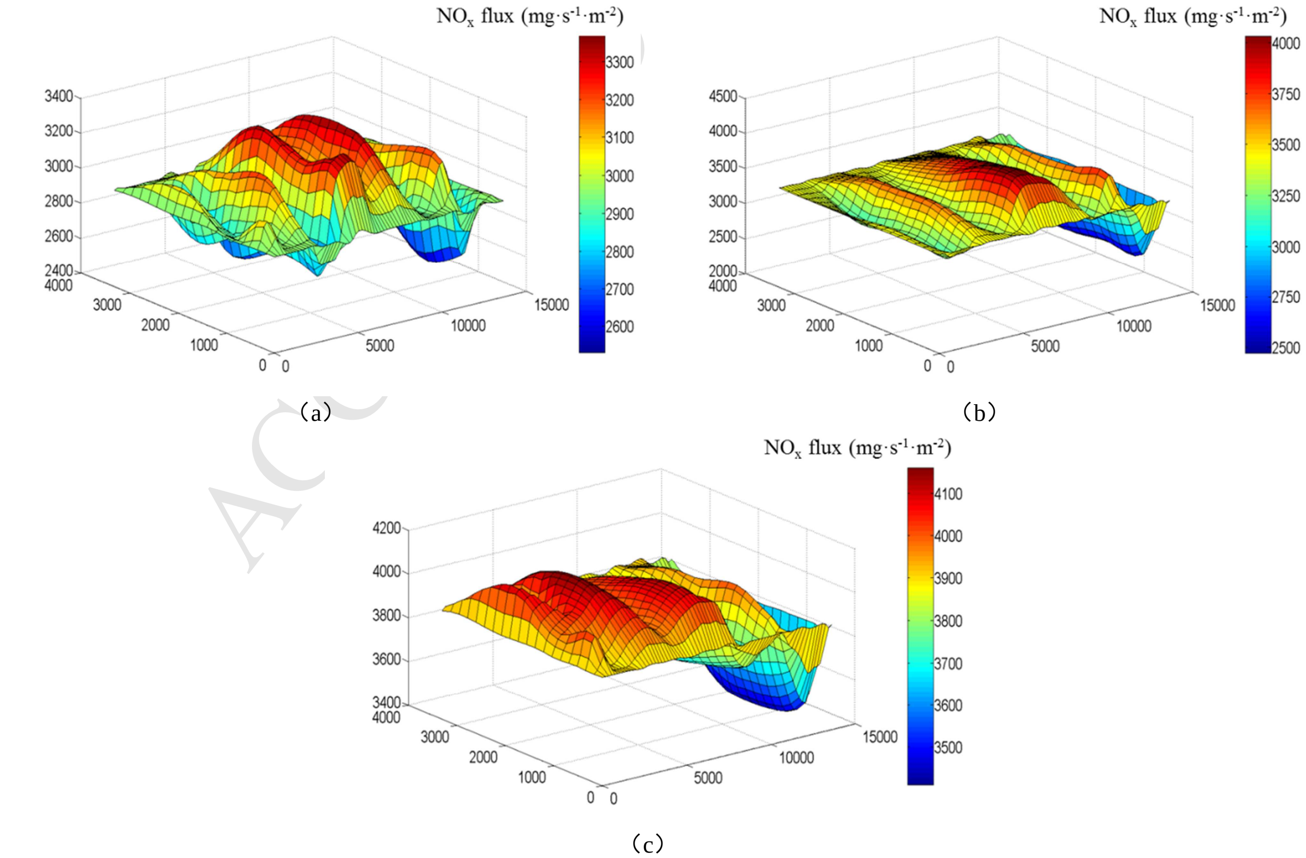

Fig. 3. The distribution of NO_x flux within cross-section A under different loads: (a) 300 MW, (b) 450MW, (c) 580MW.

It can be found that the NO_x flux within the hypothetical 27 sub-zones in line with AIG structure differed remarkably. However, an uniform NH_3 injection strategy had been applied in the above SCR system, where a poor mixing ratio of NO_x/NH_3 was destined to be maintained.

3.1.2 Analysis of the NO_x distribution within cross-section C

The serious inhomogeneity of NO_x flux at the outlet of SCR reactor could be regarded as one of the unfavorable problems caused, due to the poor matching of NO_x and NH_3. The NO_x distribution of each discrete-node within the cross-section C was obtained under 2 sets of stable load conditions including 300 and 580MW as shown in Fig. 4(a)~(b).

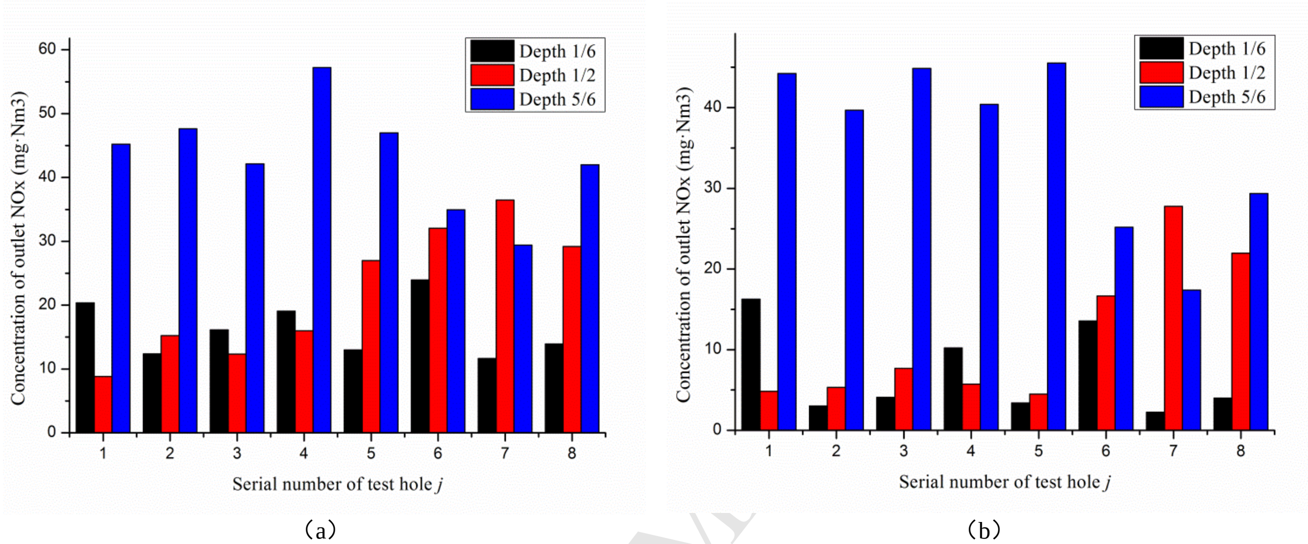

Fig. 4. The distribution of NO_x within cross-section C under different loads: (a) 300 MW, (b) 580 MW.

As can be seen from the Fig. 4, the outlet NO_x distribution had showed serious inhomogeneity with the standard deviation about 51.79% and 83.67% of 300 and 580MW load condition. The total amount of NH_3 should be excessively injected in order to ensure the maximum NO_x concentration of all discrete-nodes, such as the dimensionless depth 5/6 of test hole 5 under 580MW load condition, meeting the strict standard. As a result, the ammonia escape of the minimum emission discrete-node, such as the dimensionless depth 1/6 of test hole 7 under 580MW load condition, would be bound to significantly increase resulting in a large amount of ABS generation. Besides of that, the single point sampling method for monitoring the concentration of outlet NO_x was adopted in the continuous emission monitoring system of power plant. The measurement accuracy of NO_x concentration would be sharply reduced owing to the serious inhomogeneity of concentration distribution, which went against the safe operation of the plant.

3.2. Optimization of NH_3 injection strategy based on weight analysis

Based on the weight coefficient determined method showed in Eq (6), the weight coefficient of the 27 branch-pipes under 300, 450 and 580MW load condition was quantificationally calculated respectively according to the structure of the partition-controlled AIG system adopted showed in Fig. 2 and the distribution characteristics of NO_x flux within cross-section A showed in Fig. 3. The high, medium and low operating load conditions of the plant studied can be represented by 300, 450 and 580MW respectively. Accordingly, the load distribution characteristics of the plant studied was roughly analyzed on the basis of the operating data for 20 consecutive days as shown in Table 1.

Table 1

The load distribution of the plant within 20 consecutive days.

Load distribution interval	High load condition (≥500MW)	Medium load condition (400MW-500MW)	Low load condition (≤400MW)
Sum of time periods (ΔT^{τ})	149.5 h	121.0 h	209.5 h
Proportion	31.15%	25.21%	43.65%

Consequently, the global weight coefficient of the 27 branch-pipes for the plant studied could be obtained featuring the distribution of NO_x flux in each sub-zone under full load conditions. As shown in Fig. 5, it was easily found that global weight coefficient varied greatly for different branch-pipes. For example, the global weight coefficient of branch-pipe 5-1 was found to be the maximum reached to 1.087. Meanwhile the global weight coefficient of branch-pipe 9-1 was only about 0.760. Accordingly, the opening of the valve installed on branch-pipe 5-1 should be maintained at maximum, and the opening of the valve installed on branch-pipe 9-1 should be maintained at minimum. Only in this way can the NO_x/NH_3 mixing ratio be matched well.

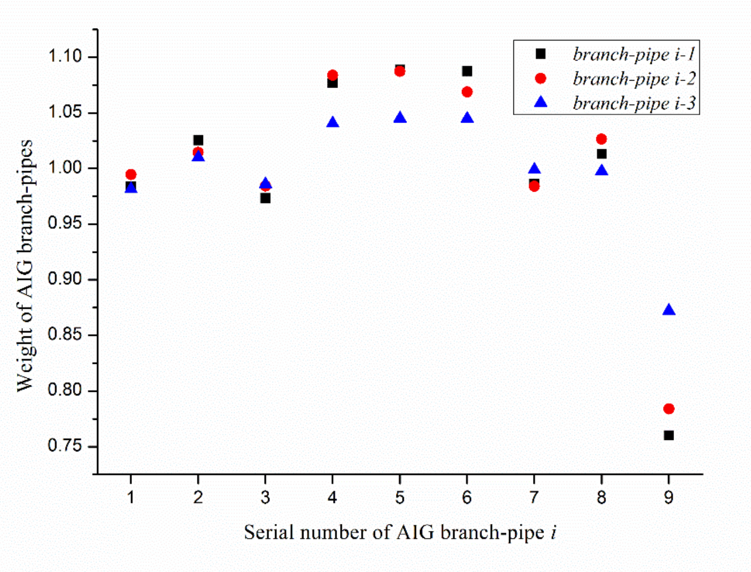

Fig. 5. The global weight coefficient of 27 branch-pipes of the SCR system.

Table 2

The strategy for NH_3 injection based on the weight analysis.

Valve numbering	1-2	2-2	3-2	4-2	5-2	6-2	7-2	8-2	9-2
	1-1	2-1	3-1	4-1	5-1	6-1	7-1	8-1	9-1
	1-3	2-3	3-3	4-3	5-3	6-3	7-3	8-3	9-3
Valve Opening (°)	56	58	54	80	80	70	54	60	39
	54	60	52	75	80	80	54	58	38
	52	58	54	65	65	65	56	56	44

The opening of AIG valves installed on each branch-pipe should be adjusted accordingly based on the weight coefficient differences and the coordination principle as shown in Eq. (8). The AIG valve used in this case had a maximum opening of 90° and a minimum opening of 0°. Moreover, the φ_{max} was found to be 1.087 and the ON_{max} was empirically assumed to be 80°. The opening of these 27 AIG valves would be kept within a reasonable range via a reasonable compression coefficient ζ, which was empirically set to 0.011 here. The optimized NH_3 injection strategy adopted could be shown in table 2.

3.3. The evaluation of the optimized NH_3 injection strategy

The application effect could be reflected through the analysis of the ammonia consumption rate, the uniformity of outlet NO_x distribution and the rising rate of the flue gas resistance of air preheater, once the optimized NH_3 injection strategy was put into use for a period.

3.3.1 The ammonia consumption rate

The ammonia consumption rate (ACR) was adopted to evaluate the application effect of the optimized ammonia injection strategy as shown in Eq. (9). It could be inferred that the higher ACR, the lower the utilization rate of ammonia and the more ammonia escape.

$$ACR = M_a / \left[\left(C_{nox}^{in} - C_{nox}^{out} \right) Q_f \right] \tag{9}$$

where M_a(mg·h^{-1}), C_{nox}^{in}(mg·Nm^{-3}), C_{nox}^{out}(mg·Nm^{-3}), Q_f(Nm^{3}·h^{-1}) represented the mass flow of ammonia consumed, the mass concentration of inlet NO_x, the mass concentration of outlet NO_x and the volume flow of flue gas, respectively.

The optimized NH_3 injection strategy was applied on the SCR system at the end of June. The ammonia consumption characteristic of the SCR system before optimization could be reflected by the average ACR in the first half of the year, which was calculated 0.420 as shown in Fig. 6.

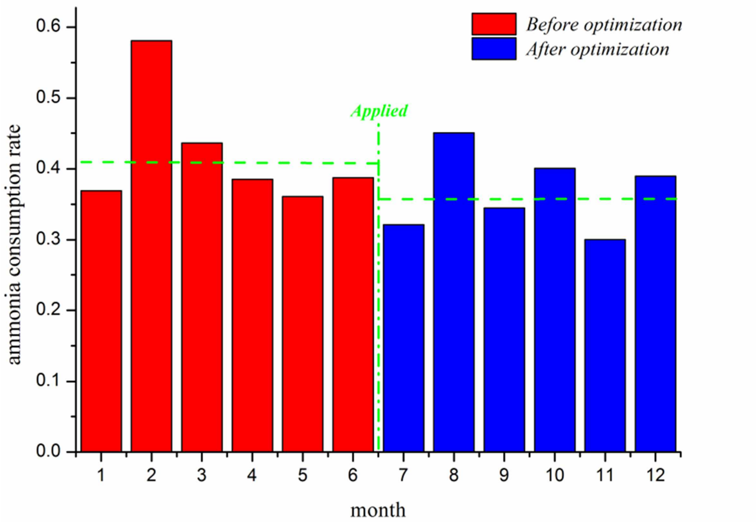

Fig. 6. The ACR before and after optimization in the case work.

However, the average ACR was reduced to 0.367 in the second half of the year after optimization. It was obvious that the average ACR of the SCR system reduced about 12.62% due to the application of the optimized NH_3 injection strategy. The occurrence of the ACR decrease could be designated to the optimization of the NO_x/NH_3 mixing ratio. The formation of ABS can be significantly confined, improving the operation performance of the plant.

3.3.2 The uniformity of the NO_x distribution of cross-section C

After the application of the optimized NH_3 injection strategy, the NO_x distribution of each discrete-node within the cross-section C was obtained again under 2 sets of stable load conditions including 300 and 580MW as shown in Fig. 7(a)~(b).

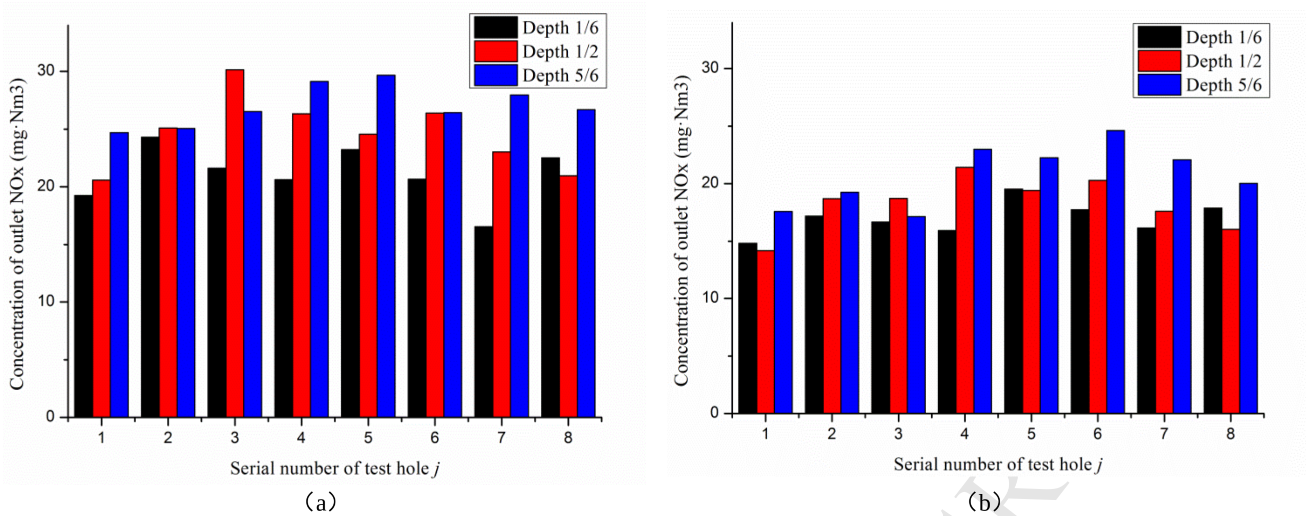

Fig. 7. The distribution of NO_x within cross-section C under different loads after optimization: (a) 300 MW, (b) 580 MW.

As can be seen from the Fig. 7, the uniformity of outlet NO_x concentration distribution was both obviously improved under 300 or 580MW load condition. The standard deviation of 300MW load condition was reduced from 51.79% to 14.27%, and the same indicator of 580MW load condition was similarly reduced from 83.67% to 14.16%. It could be calculated that the standard deviation of outlet NO_x concentration distribution would reduce from 67.73% to 14.22% with a decrease of about 79.01% after the optimization. Consequently, the total amount of ammonia could be reasonably injected to limit the ammonia escape at any discrete-node within cross-section C.

3.3.3 The rising rate of the flue gas resistance of air preheater

There is no doubt that the ammonia escape would be reduced due to the reduction of the ACR. This would help to inhibit the formation of sticky ABS on the cold side of air preheater, confining the rising rate of the flue gas resistance of air preheater.

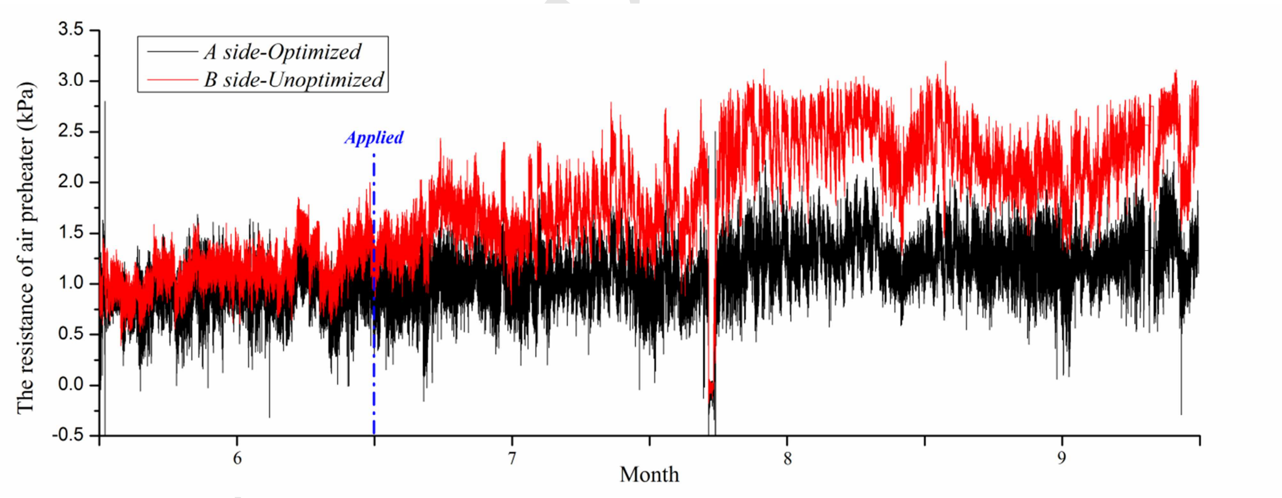

Fig. 8. The rising trend of the flue gas resistance of air preheater in the SCR system

As can be seen from the Fig. 8, the rising trend of the flue gas resistance of air preheater showed different characteristics before and after optimization. Before the application of this technology, the average resistance of A and B side was about 0.875kPa, 1.026kPa. And the monthly rising rate of these two sides was relatively low, at 11.01% and 23.06%, respectively. The rising rate has changed dramatically after the optimization. The rising rate of the flue gas resistance of A side was still increased slowly, but the increase of that of B side was obviously accelerated. According to the analysis of the three-months operation data after the optimization, the average resistance of A and B side was found to be about 1.099kPa and 1.815kPa. It should be noted that the rising rates of A side optimized increased by 14.67% and the rising rates of B side unoptimized increased by 53.85%. The rising rate of flue gas resistance could be reduced by about 39.18% due to the application of the optimized NH_3 injection technology. This implied that the formation of the sticky ABS on air preheater was significantly inhibited through the application of this technology.

4. Conclusions

A technical method for diagnosing the distribution of NO_x flux was proposed for optimizing the NO_x/NH_3 mixing ratio in SCR system of power plant. The ACR of the SCR system was reduced about 12.62% and the uniformity of outlet NOx distribution was obviously improved by about 79.01% with regard to the standard deviation after the application of the optimized NH_3 injection strategy. The rising rate of the flue gas resistance of air preheater was about 39.18% lower than that of the unoptimized side of SCR system. The formation of sticky ABS might be significantly confined with thanks to the application of this technical method.

Acknowledgements

This work was supported by the international collaboration project from Department of Science and Technology of Jiangsu Province [grant number BZ2017014].

References

[1] X. Cheng, X.T. Bi, A review of recent advances in selective catalytic NOx reduction reactor technologies, Particuology 16 (2014) 1-18.
[2] L. Dong, H. Liang, Spatial analysis on China's regional air pollutants and CO2 emissions: emission pattern and regional disparity, Atmospheric Environment 92 (2014) 280-291.
[3] T. Boningari, P.G. Smirniotis, Impact of nitrogen oxides on the environment and human health: Mn-based materials for the NOx abatement, Current Opinion in Chemical Engineering 13 (2016) 133-141.
[4] J. Hu, J. Zeng, L. Wei, Failure diagnosis and tolerant control method for hydrothermally aged SCR system by utilizing EKF observer and MRAC controller, Energy 156 (2018) 103-121.
[5] Y. Gao, T. Luan, T. LÜ, K. Cheng, H.M. Xu, Performance of V2O5-WO3-MoO3/TiO2 Catalyst for Selective Catalytic Reduction of NOx by NH3, Chinese Journal of Chemical Engineering 21(1) (2013) 1-7.
[6] C. Wu, X. Sun, B. Shen, P.T. Williams, Evaluation of carbon nanotubes produced from toluene steam reforming as catalyst support for selective catalytic reduction of NOx, Journal of the Energy Institute 87(4) (2014) 367-371.
[7] M. Shuangchen, C. Jin, J. Kunling, M. Lan, Z. Sijie, W. Kai, Environmental influence and countermeasures for high humidity flue gas discharging from power plants, Renewable and Sustainable Energy Reviews 73 (2017) 225-235.
[8] W.Z. Shi, M.M. Yang, X.H. Zhang, S.Q. Li, Q. Yao, Ultra-low emission technical route of coal-fired power plants and the cooperative removal, Zhongguo Dianji Gongcheng Xuebao/Proceedings of the Chinese Society of Electrical Engineering 36(16) (2016) 4308-4318.
[9] X. Wang, X. Du, L. Zhang, Y. Chen, G. Yang, J. Ran, Promotion of NH4HSO4 decomposition in NO/NO2 contained atmosphere at low temperature over V2O5-WO3/TiO2 catalyst for NO reduction,

Applied Catalysis A: General 559 (2018) 112-121.

[10] T. Schwämmle, F. Bertsche, A. Hartung, J. Brandenstein, B. Heidel, G. Scheffknecht, Influence of geometrical parameters of honeycomb commercial SCR-DeNOx-catalysts on DeNOx-activity, mercury oxidation and SO2/SO3-conversion, Chemical Engineering Journal 222 (2013) 274-281.

[11] Y.F. Bu, L.M. Wang, X. Chen, X.Y. Wei, L. Deng, D. Che, Numerical analysis of ABS deposition and corrosion on a rotary air preheater, Applied Thermal Engineering 131 (2018) 669-677.

[12] L. Muzio, S. Bogseth, R. Himes, Y.-C. Chien, D. Dunn-Rankin, Ammonium bisulfate formation and reduced load SCR operation, Fuel 206 (2017) 180-189.

[13] F.Y. Gao, X.L. Tang, H.H. Yi, S.Z. Zhao, C.L. Li, J. Li, Y. Shi, X. Meng, A Review on Selective Catalytic Reduction of NOx by NH3 over Mn–Based Catalysts at Low Temperatures: Catalysts, Mechanisms, Kinetics and DFT Calculations, Catalysts 7(7) (2017) 1-32.

[14] M. Zhu, J.-K. Lai, U. Tumuluri, M.E. Ford, Z. Wu, I.E. Wachs, Reaction Pathways and Kinetics for Selective Catalytic Reduction (SCR) of Acidic NOx Emissions from Power Plants with NH3, ACS Catalysis 7(12) (2017) 8358-8361.

[15] I. Malpartida, O. Marie, P. Bazin, M. Daturi, X. Jeandel, The NO/NOx ratio effect on the NH3-SCR efficiency of a commercial automotive Fe-zeolite catalyst studied by operando IR-MS, Applied Catalysis B: Environmental 113-114 (2012) 52-60.

[16] X. Liu, H. Tan, Y. Wang, F. Yang, H. Mikulcic, M. Vujanovic, N. Duic, Low NOx combustion and SCR flow field optimization in a low volatile coal fired boiler, Journal of environmental management 220 (2018) 30-35.

[17] S. Li, Z. Chen, X. Li, B. Jiang, Z. Li, R. Sun, Q. Zhu, X. Zhang, Effect of outer secondary-air vane angle on the flow and combustion characteristics and NO x formation of the swirl burner in a 300-MW low-volatile coal-fired boiler with deep air staging, Journal of the Energy Institute 90(2) (2017) 239-256.

[18] Y. Xu, Y. Zhang, F. Liu, W. Shi, J. Yuan, CFD analysis on the catalyst layer breakage failure of an SCR-DeNOx system for a 350MW coal-fired power plant, Computers & Chemical Engineering 69 (2014) 119-127.

[19] Y.Y. Xu, Y. Zhang, J. Wang, J. Yuan, Application of CFD in the optimal design of a SCR-DeNOx system for a 300MW coal-fired power plant, Computers and Chemical Engineering 49 (2013) 50-60.

[20] M.A. Buzanowski, D. Fadda, Optimized ammonia injection for power plant SCR systems, 2007 ASME Power Conference, American Society of Mechanical Engineers (2007) 493-496.

[21] C. Li, M. Shen, T. Yu, J. Wang, J. Wang, Y. Zhai, The mechanism of ammonium bisulfate formation and decomposition over V/WTi catalysts for NH3-selective catalytic reduction at various temperatures, Physical chemistry chemical physics : PCCP 19(23) (2017) 15194-15206.

[22] D. Ye, R. Qu, H. Song, X. Gao, Z. Luo, M. Ni, K. Cen, New insights into the various decomposition and reactivity behaviors of NH4HSO4 with NO on V2O5/TiO2 catalyst surfaces, Chemical Engineering Journal 283 (2016) 846-854.

[23] G.F. Liu, D.K. Shen, R. Xiao, Optimization and experimental verification of AIG tuning for SCR system of coal-fired power station based on diagnose of flow field, Dongnan Daxue Xuebao (Ziran Kexue Ban)/Journal of Southeast University (Natural Science Edition) 47(1) (2017) 98-106.

[24] H. Sjövall, L. Olsson, E. Fridell, R.J. Blint, Selective catalytic reduction of NOx with NH3 over Cu-ZSM-5—The effect of changing the gas composition, Applied Catalysis B: Environmental 64(3-4)

(2006) 180-188.
[25] L.Y. G. Ramis, G. Busca Ammonia activation over catalysts for the selective catalytic reduction of NOx and the selective catalytic oxidation of NH3. An FT-IR study, Catalysis Today 28(4) (1996) 373-380.
[26] Luca Lietti, Isabella Nova, Gianguido Ramis, Lorenzo Dall'Acqua, Guido Busca, Elio Giamello, Pio Forzatti, F. Bregani, Characterization and reactivity of V2O5-MoO3/TiO2 De-NOx SCR catalysts, Journal of Catalysis 187(2) (1999) 419-435.
[27] Z. Lei, C. Wen, B. Chen, Optimization of internals for Selective Catalytic Reduction (SCR) for NO removal, Environ Sci Technol 45(8) (2011) 3437-3444.

Journal of the Energy Institute

Highlights

- NH_3 injection strategy of AIG area was obtained via analysis of NO_x flux distribution
- Ammonia consumption rate and smoke-flow resistance rising rate was limited.
- The uniformity of outlet NO_x distribution was greatly improved.